論文 / 著書情報
Article / Book Information

Title	Empirical Study for 3D-Printed Robot Design: Dimensional Accuracy of a Hole and Proposal of a New Shaft-Fastening Method
Authors	Hiroki Kanazawa, Hiroyuki Nabae, Koichi Suzumori, Gen Endo
Citation	Proceedings of the 2022 IEEE/SICE International Symposium on System Integration, , , pp. 633-639
Pub. date	2022, 1
Copyright	(c) 2022 IEEE. Personal use of this material is permitted. Permission from IEEE must be obtained for all other uses, in any current or future media, including reprinting/republishing this material for advertising or promotional purposes, creating new collective works, for resale or redistribution to servers or lists, or reuse of any copyrighted component of this work in other works.
DOI	http://dx.doi.org/10.1109/SII52469.2022.9708832
Note	This file is author (final) version.

Empirical Study for 3D-Printed Robot Design: Dimensional Accuracy of a Hole and Proposal of a New Shaft-Fastening Method

Hiroki Kanazawa[1], Hiroyuki Nabae[1], Koichi Suzumori[1], and Gen Endo[1]

***Abstract*— 3D printing is currently being studied in many fields and is expected to be applied in the industry. However, previous studies have been based on simple evaluation models, and there have been few studies in which 3D printing technology has been evaluated after being implemented in a system. In this study, first, the existing metal robot arm was duplicated by 3D printing, and the advantages and drawbacks of implementing 3D printing were evaluated. Then, prototyping revealed that dimensional accuracy and shaft-fastening torque are significant drawbacks. Therefore we proposed and evaluated methods to address the two drawbacks of dimensional accuracy and a decrease in the shaft-fastening force of press-fitting. As for the dimensional accuracy, the tendency of the dimensional accuracy was investigated quantitatively by manufacturing several samples of the hole shape and measuring the dimensional accuracy. To address the decrease in the shaft-fastening torque of press-fitting, a new shaft fastening method using hexagonal metal parts and a hexagonal 3D printed hole was proposed. It was experimentally verified that the proposed mechanism could achieve sufficient torque capacity.**

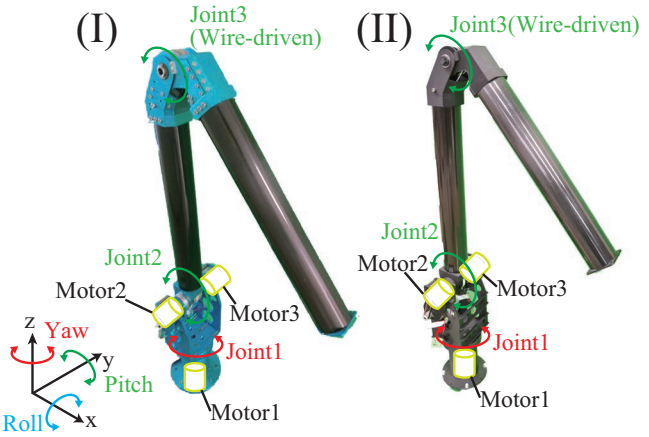

Fig. 1. Three-degree-of-freedom robot arm made of (I)metal and (II)3D printed CFRP: elbow joint(J3) is driven by wires.

I. INTRODUCTION

The world is in the midst of "Industrie 4.0," and social manufacturing is expected to be one of the most representative approaches, in which industrial machines are connected to the Internet and anyone in the world can participate in design and manufacturing [1]. 3D printing has been considered as a core technology to achieve social manufacturing. It is a technology that converts 3D shape data created by computer aided design(CAD) software into a stack of 2D cross-sections to produce an object with approximately the same original shape data. Because 3D printing can be applied to a wide range of materials such as polymers, metals, ceramics, cement, and because functions such as electrical conductivity can be added by mixing nanoparticles into the polymer [2], it is being actively researched not only in the mechanical field but also in the architectural and electrical fields [3]–[7]. Various layering methods have been proposed for 3D printing, such as fused deposition modeling(FDM), selective laser melting(SLM), stereolithography (SLA), electron beam melting (EBM), and material jetting [8]. Among them, FDM is the most widespread because of its low cost and the availability of materials.

When 3D printing is used in industry, there are great economic benefits such as increased product value through mass-customization and shortened time to market through rapid prototyping [9]–[12]. In contrast, 3D printing has problems related to the anisotropy of material strength and dimensional accuracy [8], [13], which hinder its industrial application. For material strength, there have been some studies on tensile tests using simple models [14], strengthening structurally weak parts by changing the internal density [15], and creating a database using strength simulation [16]. Several methods have been proposed to print with as few support structures as possible in FDM and SLA [17]–[19]. In addition, many studies conducted on minimizing the amount of materials used while maintaining the strength of the part by using topology optimization [20], [21]. However, these studies are often simple evaluation models or studies of a certain part of an application, and there have been few studies that have evaluated problems and presented systematic solutions through manufacturing the entire robot mechanism by 3D printing.

Therefore, in this study, the advantages and drawbacks of 3D printing were addressed by replacing the metal structural parts of a three-degree-of-freedom(3-DOF) lightweight robot arm with 3D-printed plastic parts (Section II). The 3-DOF arm was originally designed by utilizing a cutting process and sheet metal bending process. Then, the following drawbacks revealed are discussed in detail.

- Dimensional accuracy: Because the accuracy of parts made by 3D printing is generally low, we aim to establish a method to modulate the target size of the

[1]All authors are with the Department of Mechanical Engineering, Tokyo Institute of Technology, 2-12-1 Ookayama, Meguroku, Tokyo 152-8550,Japan. nabae@mes.titech.ac.jp

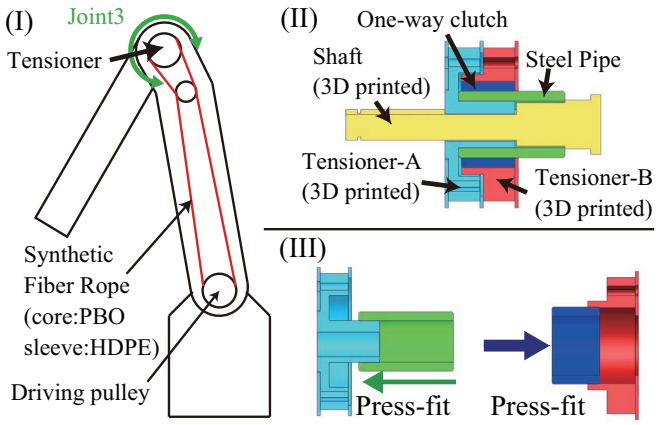

Fig. 2. (I)Conceptual diagram of the wire-driven mechanism for Joint3. Tensioner mechanism is installed at Joint3. (II)Detail of tensioner mechanism. (III)One-way clutch was press-fitted into Tensioner-B, and Steel Pipe was press-fitted to Tensinoer-A.

parts at the design stage. In this paper, the hole shape was evaluated quantitatively (Section III).

- Low shaft-fastening torque by press-fit: Press-fit is a widely used fastening method in mechanical design because it does not require other fastening parts and is easy to reduce the cost. However, if one uses 3D-printed parts that have inferior material strength, press-fitting does not function because it depends on the strength of the material. Therefore, we propose a new fastening method for 3D printed parts that can be used with press-fitted parts (Section IV).

II. Prototype and Evaluation of 3D Printed Robot Arm

A. 3D-printed 3-DOF wire-driven robot arm

Figure 1 shows the modeled metal 3-DOF manipulator and 3D-printed robot arm manufactured in this study. In this manipulator, the root axis (Joint1, J1) rotates in the yaw direction, while the shoulder joint (Joint2, J2) and the elbow joint (Joint3, J3) of the arm rotate in the pitch direction. At J1 and J2, the output of the motor is input to the wave gear reducer and directly drives the joints. J3 is driven by transmitting the output of the wave gear reducer to the wire-pulley system and maintaining the tension by the tensioner mechanism. As shown in Fig. 2, the tensioner mechanism consists of pulleys, a shaft, and a one-way clutch. The one-way clutch limits the free rotation of the pulleys only to the direction of increasing tension, and the structure transmits the rotation of the drive pulley to the axis of the J3 joint.

In prototyping the 3D printed robot arm, only the metal structural parts were replaced with 3D-printed parts, and the functional components (motors, reducers, and bearings) and fastening components were commercially available. This was done to evaluate the effects of stiffness and weight when replacing the structural parts with those made by 3D printing, and to eliminate the effects of elements that may change the function itself when manufactured by 3D printing. However, because the aforementioned tensioner mechanism requires a hard shaft owing to the principle of the one-way clutch, it was made to function by press-fitting a steel pipe into the plastic shaft only at the part where it interacts with the one-way clutch. The structural parts were made from thermoplastic carbon fiber reinforced plastic(CFRP) using Markforged Mark Two and X7, Onyx (finely chopped carbon fiber kneaded into polyamide provided by Markforged), and a continuous carbon fiber. In addition, in order to improve the efficiency of assembly work and shorten the modeling time, some parts that consisted of multiple structural parts and many fastening parts in the model metal arm were combined and made as a single part by using 3D printer. Consequently, we succeeded in significantly reducing the total number of parts and assembly time.

B. Evaluation of dimensional accuracy

Generally, 3D-printed parts are considered to have low accuracy [8]. In the case of the parts of the robot arm manufactured in this study, the dimensional accuracy of the holes for the screws, bearings, and axes was not sufficient, and additional processing, such as sanding, was required. Essentially, the use of parts made by 3D printers should lead to a reduction in machining cost and material loss because the finished parts can be assembled without additional work. However, if the dimensional accuracy remains low, additional processing is required, making industrial applications difficult. Therefore, it is necessary to improve the dimensional accuracy, but this is difficult because additive machining is considered to be less accurate than cutting in principle. Therefore, it is necessary to understand the extent of dimensional errors when a part is manufactured using a 3D printer. If errors can be predicted in advance, we can reflect the deviation in the design or cancel it when generating tool paths for 3D printing.

C. Evaluation of joint stiffness

The siffness of each joint was measured to evaluate the performance of the robot arm. The joint stiffness was measured for J2 and J3 joints according to the static compliance measurement defined in JIS B 8432:1999 (ISO 9283:1998). J1 was not measured because the stiffness depends on the stiffness of the material and bearing rather than on the structure of the mechanism and is easy to predict. The equipment made is shown in Fig. 3. A load was applied to the tip of the arm. The load is applied by the 10 % of the rated load up to 100% in both positive and negative directions parallel to the xyz-axis of the base coordinate system respectively, and the displacement was measured as the load was increased. In this experiment, 100 % of the rated load was 506 g (=4.96 N). However, when the displacement was too large for the equipment, the weight used for the load touched the ground. In the case of J2 in the z-direction, it was not possible to obtain data for this reason. Therefore, the robot was rotated 90 degree clockwise, as shown in Fig. 3 (I)-b, so as not to touch the ground, and the joint stiffness was measured. To measure the stiffness of each

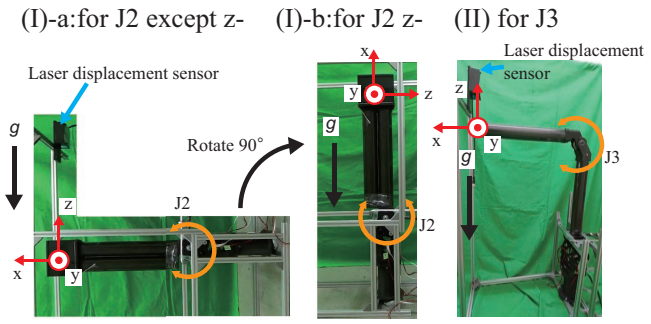

Fig. 3. Test equipment for static compliance.

TABLE I

ABSOLUTE VALUE OF STATIC COMPLIANCE AT EACH JOINT.

J2 [mm/N]	x+	x-	y+	y-	z+	z-
3D printed arm	0.499	0.0208	1.04	0.908	3.96	1.82
Metal arm	0.392	-	0.210	0.172	0.894	0.262
J3 [mm/N]	x+	x-	y+	y-	z+	z-
3D printed arm	0.395	0.164	1.95	1.98	67.0	60.3
Metal arm	0.407	0.375	0.504	0.524	8.06	4.91

joint in this experiment, all the joints except the joint to be measured were fixed to an aluminum frame. However, the x-axis direction of the metal arm could not be measured owing to the configuration of the equipment.

Table I shows the joint stiffness values. For both J2 and J3 , there was no significant difference in the x-axis load between the metal and 3D printing arms, and for J3, the 3D-printing arm showed slightly better results. However, the stiffness of the 3D-printed arm was much lower than that of the metal arm in the y- and z-axes. Especially in the z-axis direction of J3, the 3D-printed arm could not hold the load. It was caused by a problem in the transmission mechanism.

One possible cause is the tensioner of the wire drive system. As mentioned above, J3 is equipped with a tensioner, as shown in Fig. 2, which can maintain the tension of the wire. Tensioner-B and the One Way Clutch, and Tensioner-A and the Steel Pipe are assembled by press fitting. Therefore, it is considered that slippage occurs on the press-fitted surface. Because the surface of the 3D-printed parts is soft, the fastening strength of the 3D-printed parts is considered to be much lower than that of the press-fitted parts on the metal. Therefore, it is necessary to change the fastening method.

III. IDENTIFYING TENDENCY IN DIMENSIONAL ACCURACY

Increasing the dimensional accuracy of parts made using an FDM 3D printer is fundamentally difficult. This is because, when the molten material is ejected from the nozzle, the material is deposited while being pressed against the modeling surface, so the ejected material is crushed, and the material inevitably becomes larger than the nozzle diameter. Therefore, it is hypothesized that there is a certain tendency in the deviation of the dimensional accuracy, and an attempt was made to predict the deviation of the dimensional

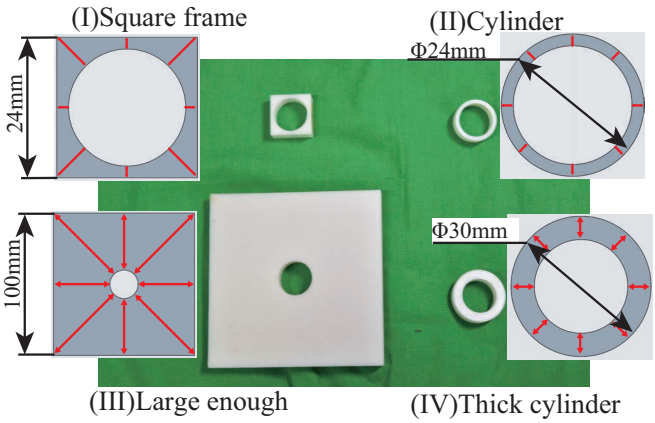

Fig. 4. Samples used for measurements. Ten of each of these were printed on three different 3D printers.

accuracy in advance by understanding the tendency. In the prototyping of the robot arm described in the previous section, the parts that required additional processing were the shaft and the hole, such as the hole for the screw, the bearing, and the shaft. These are typical geometrical shapes in the mechanical design of robots. Therefore, in this study, an attempt was made to understand the tendency of the dimensional accuracy of the holes that often exist in the structural members.

A. Change in shape accuracy caused by difference in wall thickness

1) Details of the measurement sample: 3D-printed parts are affected by thermal shrinkage because the polymer is heated to more than 200 ° C during the molding process.

However, the extent to which the dimensions are affected by the thermal shrinkage has not been clarified. Therefore, in this study, the tendency of the thermal shrinkage to affect the dimensions wa investigated by changing the wall thickness around the holes. In 3D printing, the polymer is extruded with a thin nozzle, so there are two types of structure: an outer shell and an inner filling structure that bridges the outer shells. The purpose of this experiment was to understand the influence of thermal shrinkage and internal structure.

The shapes of the measured samples are shown in Fig. 4. The direction of the 3D printing was perpendicular to the paper surface, and 10 samples of each were prepared using a the 3D printer. The 3D printer and materials were Zortrax M-200 and ABS resin Z-ULTRAT by Zortrax, X7 and Onyx by Markforged, and Raise3d Pro2 and genuine PLA by Raise 3D Technologies, Inc. After molding, a contact-type coordinate measuring machine(CMM) (TESA micro-hite 3D, manufactured by TESA Technology) was used to measure three characteristics: dimensional error, roundness, and cylindricity. The dimensional error is defined as the deviation from the target value (ϕ20 mm) obtained by averaging the circumferential trajectory of the hole obtained by the CMM. However, all the dimensional errors were all negative, i.e., all the samples have holes with a smaller diameter than the

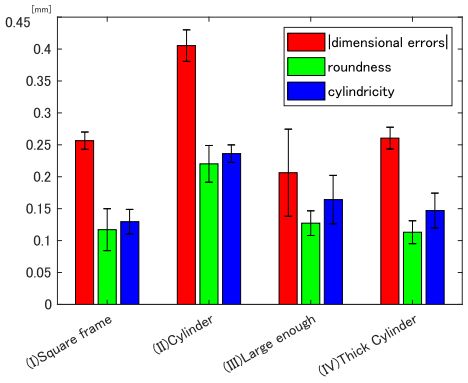

Fig. 5. Result of Zortrax M-200 with Z-ULTART.

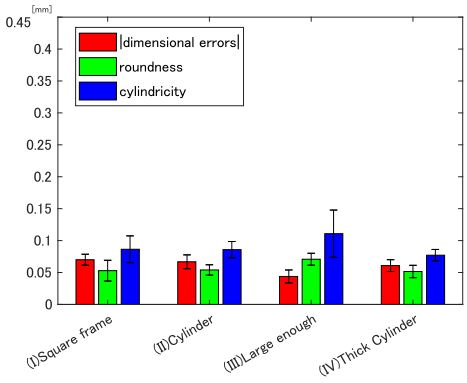

Fig. 7. Result of Raise 3D Pro2 with PLA.

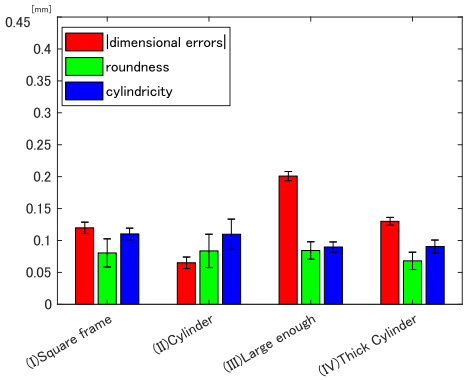

Fig. 6. Result of Markforged X7 with Onyx.

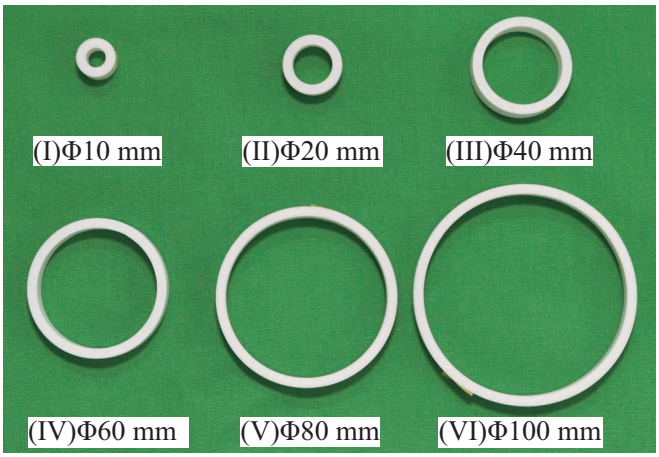

Fig. 8. Samples used for measurements.

target value, so they are described in absolute values in the graph. The values of roundness and cylindricity are the same as those defined in JIS B 0419:1991 (ISO 2768-2:1989).

The samples shown in Fig. 4 all have holes of ϕ20 mm and the surrounding frames are different. Frames (I), (II), and (III) are squares, circles, and sufficiently large squares, respectively, to investigate the effect of thermal shrinkage resulting from non-uniform wall thickness. If the effect of thermal shrinkage on the dimensional accuracy is large, geometric tolerance values such as roundness and cylindricity are expected to be large. On the other hand, because the amount of thermal shrinkage is determined as a percentage of the part dimensions, the dimensional error is expected to be largest for (III), which has the largest wall thickness. Frames (II) and (IV) have the same cylindrical shape; however the wall thickness is different. In (II), the target shape is not formed because of the small wall thickness, and the contact between the infill and the shell is not uniform. Therefore the effect of the difference in the internal shape is discussed.

2) Results: Figures 5-7 show graphs obtained from the measurements. Focusing on Fig. 5, the thin-walled cylinder of (II) were less accurate than those of (I), (III), and (IV) in all indices. Therefore, the effect of thermal shrinkage on Zortrax M-200 and Z-ULTRAT is small, and the uniformity of the infill structure has a significant influence on the dimensional accuracy of the holes. On the other hand, the dimensional errors in Fig. 6 reveal that the thin-walled cylinder in (II) has the smallest error, although it is slight, and the errors in (I) and (IV) are almost the same, while (III) has the largest. Namely, for Markforged X7 and Onyx, the larger the maximum wall thickness, the larger the dimensional error, which indicate that they are greatly affected by thermal shrinkage. Finally, as shown in Fig. 7, the dimensional error, roundness, and cylindricity of all samples are similar, so it is considered that the samples are not affected by the difference in wall thickness.

As described above, the tendency of the dimensional accuracy varies greatly depending on the combination of the 3D printer and material. However, if the target diameter is ϕ20 mm, then we should enlarge the 3DCAD model to 20.4, 20.2, 20.1 for Zortrax M-200, Markforged X7, and Raise3D, respectively. Even when such characteristics are unknown, shapes with non-uniform internal shapes, such as (II), or with large maximum wall thickness, such as (III), should be avoided because they may reduce the dimensional accuracy.

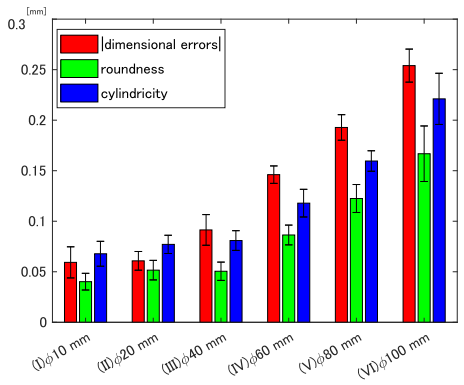

Fig. 9. Change in accuracy when hole diameter is changed

B. Change in shape accuracy caused by change in hole diameter

1) Details of the measurement sample: In the cutting process, the larger the target size, the larger the set value of general tolerance. Therefore, how the change of the hole diameter affects the dimensional accuracy in the case of 3D printing was investigated.

The shapes of the measured samples are shown in Fig. 8. Each of the 10 samples was made using Raise3D and PLA, and the shape accuracy was measured in the same way as described in the previous section.

2) Results: Figure 9 shows a graph obtained from the measurements. For hole diameters larger than (II)ϕ20 mm, the accuracy of all indices decreased as the hole diameter increased, as in the case of cutting. In addition, because the decrease in accuracy is almost linear, it is easy to predict the molding accuracy for hole diameters other than those measured in this study. Therefore, one can predict the fabrication accuracy of the 3D printer at the design stage by measuring the tendency of the dimensional accuracy of three samples from among (II) to (VI).

On the other hand, there was almost no change between (I)ϕ10 mm and (II)ϕ20 mm. This means that there is an upper limit on the dimensional accuracy. In the FDM method, the extruded material spreads and stacks larger than the diameter of the nozzle; therefore, a part of the material protrudes inward from the trajectory of the nozzle when a hole is drawn. Because the amount of polymer that protrudes is considered to be constant for the same 3D printer with the same settings, it becomes the upper limit of dimensional accuracy. Because it is necessary to understand this upper limit for design, it is desirable to measure it beforehand and understand the characteristics of the 3D printer.

IV. Proposal of a New Component Configuration for Press Fitting

Because press-fitting is a fastening method that depends on the surface hardness of the parts, it is difficult to achieve with FDM 3D-printed parts, which are supposed to be made from polymer. However, because there are many parts made on the premise of press-fitting, press-fitting is necessary for industrial applications. Therefore we focused on the high flexibility in shape of 3D printers. Because 3D printers are a method of adding material to an existing object, they can create polygonal holes that cannot be created by cutting. Therefore, the aim was to achieve press-fit fastening by using structural constraint with geometrical shapes using polygons. In addition, this method is verified using the tensioner mechanism of the wire-driven system, and the applicability to the wire-driven robot arm was evaluated quantitatively.

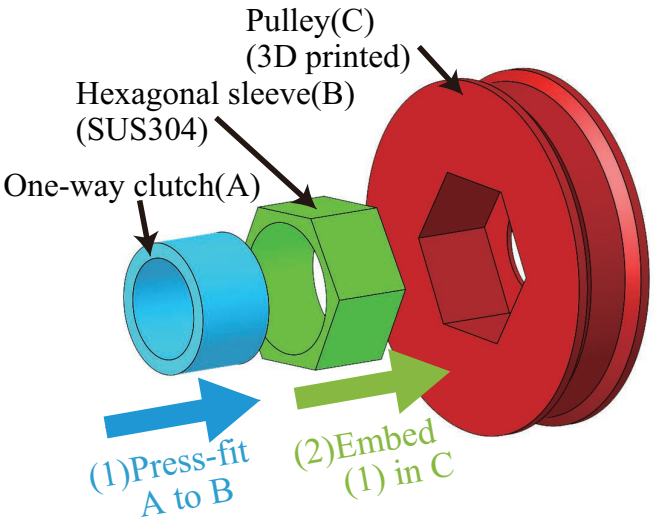

Fig. 10. Design concept of tensioner.

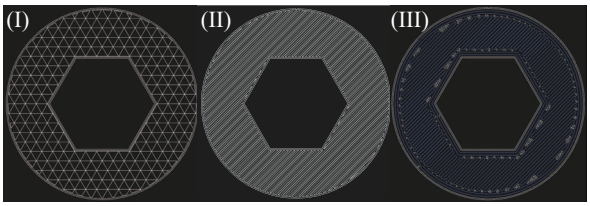

Fig. 11. Types of infill structure: white line is Onyx, and blue line is continuous carbon fiber.

A. Design concept

Figure 10 shows the design concept of the tensioner mechanism for verification. The tensioner mechanism consists of two parts in one set: a mechanism to maintain tension with a press-fitted one-way clutch, and a mechanism to transmit the torque to the shaft. However, the tensioner mechanism with a press-fitted one-way clutch was only used for verification. The one-way clutch was press-fitted into a metal sleeve with a hexagonal outer surface, and the sleeve was fitted into a 3D printer part with a hexagonal hole to constrain the rotation of the one-way clutch around the axis. Because the press-fitted part was a metal-to-metal fastening, the same fastening force as a normal press-fit was expected.

B. Tension load test

The conceptual model was prototyped, and an experiment was conducted to determine the extent to which tension could

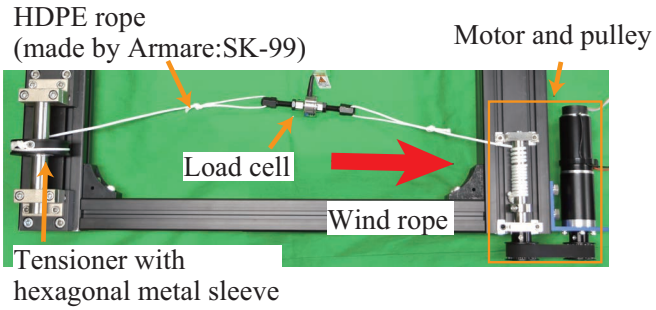

Fig. 12. Equipment for tension loading: load cell is used to measure the tension of the rope.

be applied. The 3D-printed parts were made using Markforged MarkTwo and Onyx. Three types of infill structures also manufactured, as shown in Fig. 11:(I) an Onyx-only structure with a triangular hole and a filling ratio of 37%, (II) an Onyx-only structure with a filling ratio of 100%, and (III) a structure with a filling ratio of 100% and reinforced with continuous carbon fiber. The results were compared. Using the equipment shown in Fig. 12, tensions of 0.5, 1.0, 1.5, and 1.7 kN were applied step by step, and the rope tension was measured with a load cell. Here, 1.7 kN is twice the limit value of the tension calculated from the torque capacity of the one-way clutch.

Figure 13 shows an example of the experimental results. This result is for the modeling condition shown in Fig. 11(I), and other results are omitted because the results for the other printing conditions were similar. Finally, a tension exceeding the torque capacity of the one-way clutch was applied when a current equivalent to 1.7 kN was applied to the motor. In addition, no significant deformation of the 3D-printed parts or slippage on the press-fit surface was observed during the experiment. On the other hand, the tension increased immediately after the current command value was changed and then decreased gradually. This is considered to result from the viscoelasticity of the synthetic fiber rope, as shown in the literature [22]. The above demonstrates that this method is very effective for mounting press-fit parts on robots made by 3D printers.

C. Performance evaluation with a robot arm

The effectiveness of the proposed method was verified by implementing the tensioner mechanism described in this section to the robot arm described in Section II and comparing the performance. The joint stiffness was measured using the apparatus described in Section II. Only the ±z direction of the J3 joint, which is considered to be caused by the tensioner mechanism, was measured for comparison. The experimental results are shown in Table II. A significant improvement in the joint stiffness is observed in both ±Z directions. The joint stiffness of the 3D printer robot arm was still lower than that of the metal arm, however this is probably caused by the stiffness of the other structural components. Because the robot arm was designed to be made of metal, it is expected that the stiffness of the polymer, which has a low

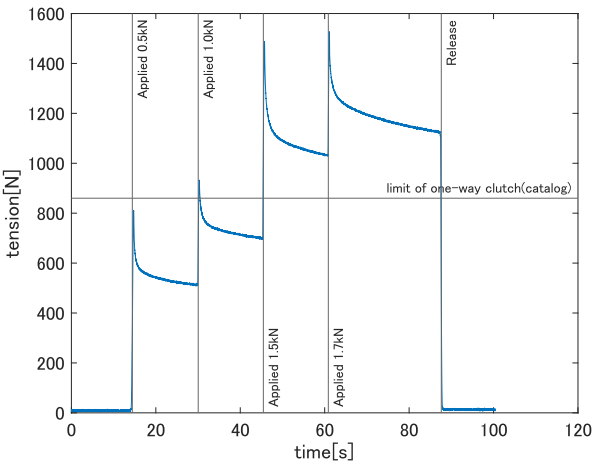

Fig. 13. Measured tension when tension was applied to the concept model.

TABLE II
THE ABSOLUTE VALUE OF STATIC COMPLIANCE AT J3 JOINT.

J3 [mm/N]	z+	z-
3D printed arm	67.0	60.3
Metal arm	8.06	4.91
3D printed arm (with hexagonal metal sleeve)	11.5	13.9

Young's modulus, was insufficient. Therefore, it is expected that the robot arm can be improved if it is designed to be manufactured using a 3D printer.

V. CONCLUSIONS

In this study, the structual parts of the existing metal robot arm were replaced with 3D-printed parts and clarified the problems that were not apparent in the previous studies. Then, to solve the problem of dimensional accuracy, samples of the hole shape were manufactured, and the dimensional accuracy was measured to understand the tendency. The accumulation of such data will make it possible to predict the dimensional deviation in advance. In addition, we proposed and confirmed the effectiveness of the new press-fitting method by partially replacing the press-fitted part with metal and using geometric shapes to fasten the 3D-printed parts.

In the future, since economic efficiency is also important for industrial use, it is necessary to evaluate the economic efficiency of the proposed method. Moreover, it is planned to design a robot arm assuming that it will be manufactured using a 3D printer, and we aim to develop a robot arm with sufficient functions for industrial use.

ACKNOWLEDGMENT

This research is subsidized by New Energy and Industrial Technology Development Organization (NEDO) under a project JPNP20016. This paper is one of the achievements of joint research with and is jointly owned copyrighted material of ROBOT Industrial Basic Technology Collaborative Innovation Partnership.

REFERENCES

[1] J. Wan, H. Cai, and K. Zhou, "Industrie 4.0: Enabling technologies," in *Proceedings of 2015 International Conference on Intelligent Computing and Internet of Things*, 2015, pp. 135–140.

[2] X. Wang, M. Jiang, Z. Zhou, J. Gou, and D. Hui, "3d printing of polymer matrix composites: A review and prospective," *Composites Part B: Engineering*, vol. 110, pp. 442–458, 2017. [Online]. Available: https://www.sciencedirect.com/science/article/pii/S1359836816321230

[3] A. Albar, M. R. Swash, and S. Ghaffar, "The design and development of an extrusion system for 3d printing cementitious materials," in *2019 3rd International Symposium on Multidisciplinary Studies and Innovative Technologies (ISMSIT)*, 2019, pp. 1–5.

[4] Z. Liu, W.-D. Li, Y.-B. Wang, G.-Q. Su, G.-J. Zhang, Y. Cao, and D.-C. Li, "Topology optimization and 3d-printing fabrication feasibility of high voltage fgm insulator," in *2016 IEEE International Conference on High Voltage Engineering and Application (ICHVE)*, 2016, pp. 1–4.

[5] C. M. Shemelya, M. Zemba, M. Liang, D. Espalin, C. Kief, H. Xin, R. Wicker, and E. W. MacDonald, "3d printing multi-functionality: Embedded rf antennas and components," in *2015 9th European Conference on Antennas and Propagation (EuCAP)*, 2015, pp. 1–5.

[6] A. Delage, N. Delhote, S. Verdeyme, B. Bonnet, L. Carpentier, C. Schick, T. Chartier, and C. Chaput, "Aerosol jet printing of millimeter wave transmission lines on 3d ceramic substrates made by additive manufacturing," in *2018 IEEE/MTT-S International Microwave Symposium - IMS*, 2018, pp. 1557–1560.

[7] E. Macdonald, R. Salas, D. Espalin, M. Perez, E. Aguilera, D. Muse, and R. B. Wicker, "3d printing for the rapid prototyping of structural electronics," *IEEE Access*, vol. 2, pp. 234–242, 2014.

[8] F. Calignano, D. Manfredi, E. P. Ambrosio, S. Biamino, M. Lombardi, E. Atzeni, A. Salmi, P. Minetola, L. Iuliano, and P. Fino, "Overview on additive manufacturing technologies," *Proceedings of the IEEE*, vol. 105, no. 4, pp. 593–612, 2017.

[9] B. Berman, "3-d printing: The new industrial revolution," *Business Horizons*, vol. 55, no. 2, pp. 155–162, 2012. [Online]. Available: https://www.sciencedirect.com/science/article/pii/S0007681311001790

[10] T. H. M. Siddique, I. Sami, M. Z. Nisar, M. Naeem, A. Karim, and M. Usman, "Low cost 3d printing for rapid prototyping and its application," in *2019 Second International Conference on Latest trends in Electrical Engineering and Computing Technologies (INTELLECT)*, 2019, pp. 1–5.

[11] F. G. Sisca, C. M. Angioletti, M. Taisch, and J. A. Colwill, "Additive manufacturing as a strategic tool for industrial competition," in *2016 IEEE 2nd International Forum on Research and Technologies for Society and Industry Leveraging a better tomorrow (RTSI)*, 2016, pp. 1–7.

[12] C. Weller, R. Kleer, and F. T. Piller, "Economic implications of 3d printing: Market structure models in light of additive manufacturing revisited," *International Journal of Production Economics*, vol. 164, pp. 43–56, 2015. [Online]. Available: https://www.sciencedirect.com/science/article/pii/S0925527315000547

[13] T. D. Ngo, A. Kashani, G. Imbalzano, K. T. Nguyen, and D. Hui, "Additive manufacturing (3d printing): A review of materials, methods, applications and challenges," *Composites Part B: Engineering*, vol. 143, pp. 172–196, 2018. [Online]. Available: https://www.sciencedirect.com/science/article/pii/S1359836817342944

[14] F. van der Klift, K. Yoichiro, T. Akira, U. Masahito, H. Yoshiyasu, and M. Ryosuke, "3D Printing of Continuous Carbon Fibre Reinforced Thermo-Plastic (CFRTP) Tensile Test Specimens," *Open Journal of Composite Materials*, vol. 6, no. 1, pp. 18–27, 2016.

[15] D. Li, N. Dai, X. Jiang, Z. Shen, and X. Chen, "Density aware internal supporting structure modeling of 3d printed objects," in *2015 International Conference on Virtual Reality and Visualization (ICVRV)*, 2015, pp. 209–215.

[16] M. H. Ali, G. Yerbolat, and S. Amangeldi, "Material optimization method in 3d printing," in *2018 IEEE International Conference on Advanced Manufacturing (ICAM)*, 2018, pp. 365–368.

[17] G. Fazzini, P. Paolini, R. Paolucci, D. Chiulli, G. Barile, A. Leoni, M. Muttillo, L. Pantoli, and G. Ferri, "Print on air: Fdm 3d printing without supports," in *2019 II Workshop on Metrology for Industry 4.0 and IoT (MetroInd4.0 IoT)*, 2019, pp. 350–354.

[18] X. Wei, S. Qiu, L. Zhu, R. Feng, Y. Tian, J. Xi, and Y. Zheng, "Toward support-free 3d printing: A skeletal approach for partitioning models," *IEEE Transactions on Visualization and Computer Graphics*, vol. 24, no. 10, pp. 2799–2812, 2018.

[19] J. Vanek, J. A. G. Galicia, and B. Benes, "Clever support: Efficient support structure generation for digital fabrication," *Computer Graphics Forum*, vol. 33, no. 5, pp. 117–125, 2014. [Online]. Available: https://onlinelibrary.wiley.com/doi/abs/10.1111/cgf.12437

[20] G. Yongxin, Z. Lihua, L. Zhijia, G. Yimin, and M. Lingxi, "Optimization design of star tracker bracket of small satellite for 3d printing," in *2019 5th International Conference on Control, Automation and Robotics (ICCAR)*, 2019, pp. 808–811.

[21] I. Chavdarov and B. Naydenov, "Software application for topology optimization of a link from a 3d printed educational robot," in *2020 International Conference on Software, Telecommunications and Computer Networks (SoftCOM)*, 2020, pp. 1–6.

[22] A. Takata, G. Endo, K. Suzumori, H. Nabae, Y. Mizutani, and Y. Suzuki, "Modeling of synthetic fiber ropes and frequency response of long-distance cable-pulley system," *IEEE Robotics and Automation Letters*, vol. 3, no. 3, pp. 1743–1750, 2018.